Side chain engineering of mono-fluorinated acceptors for efficient non-halogenated solvent-processed organic solar cells

Mei Luo,*[a] Siyu Zhao,[b] Lingchen Kong,[b] Zesheng Zhang,[b] Jialong Xie,[b] Xuanchen Liu,[b] and Junwu Chen,*[b]

[a]College of Chemical and Biological Engineering

Hunan University of Science and Engineering

Yongzhou 425199, China

E-mail: lmei@huse.edu.cn

[b] Institute of Polymer Optoelectronic Materials and Devices

Guangdong Basic Research Center of Excellence for Energy and Information Polymer Materials

State Key Laboratory of Luminescent Materials and Devices

South China University of Technology

Guangzhou 510640, P. R. China

E-mail: psjwchen@scut.edu.cn

Supplementary data

Experimental Section

Materials

All solvents and reagents were used as received from commercial sources and used without further purification unless otherwise specified. Compound $BTzC_4C_{12}$-2CHO synthesized according to the previous report.[1]

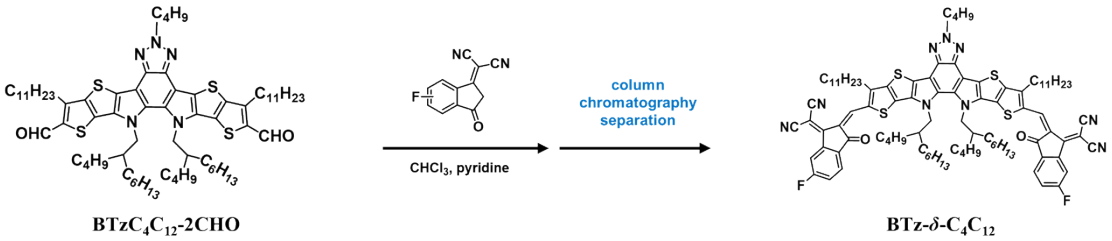

Scheme S1. Synthetic route for **BTz-*δ*-C_4C_{12}**.

BTzC$_4$C$_{12}$-2CHO.^{1}H NMR (400 MHz, chloroform-*d*) δ (ppm): 10.13 (s, 2H), 4.83 (d, *J*=7.5 Hz, 2H), 4.60 (d, *J*=7.9 Hz, 4H), 3.19 (t, *J*=7.8 Hz, 4H), 2.21 (td, *J*=7.2, 3.6 Hz, 4H), 1.89–1.78 (m, 8H),1.55–1.29 (m, 24H), 1.07–0.75 (m, 34H), 0.72–0.49 (m, 25H).

BTz-δ-C$_4$C$_{12}$. ^{1}HNMR (400 MHz, chloroform-*d*) δ (ppm): 9.16 (s, 2H), 8.40 (dd, *J* = 9.1, 2.1 Hz, 2H), 7.93 (dd, *J* = 8.3, 5.2 Hz, 2H), 7.42 (td, *J* = 8.2, 2.1 Hz, 2H), 4.92 – 4.62 (m, 6H), 3.22 (t, *J* = 7.9 Hz, 4H), 2.21 (p, *J* = 7.5 Hz, 2H), 2.06 (p, *J* = 6.6 Hz, 2H), 1.88 (p, *J* = 7.7 Hz, 4H), 1.63–1.42 (m, 8H), 1.40–1.22 (m, 29H), 1.14–0.81 (m, 35H), 0.74–0.47 (m, 16H). ^{13}CNMR (101MHz, chloroform-*d*) δ (ppm):187.06, 167.89, 165.33, 159.66, 142.43, 142.33, 133.56, 133.10, 129.60, 129.58, 125.53, 125.43, 124.81, 121.47, 121.24, 115.29, 114.73, 112.83, 112.57, 111.76, 68.28, 56.17, 55.36, 39.03, 32.32, 31.56, 31.25, 30.45, 30.36, 30.30, 30.20, 29.87, 29.66, 29.62, 29.53, 29.51, 29.40, 29.35, 22.83, 22.77, 22.48, 22.46, 19.98, 14.13, 14.03, 13.78, 13.66. HR-MS (MALDI-TOF): m/z calcd. For ($C_{94}H_{113}F_2N_9O_2S_4$): 1567.24 Found: 1468.6328.

General characterizations

^{1}HNMR spectra, and ^{13}C NMR spectra were recorded on a Bruker AV 400 spectrometer with tetramethylsilane (TMS) as the internal reference. Mass spectrometer (MALDI-TOF) was performed on a Autoflex III smart bean. Elemental analyses were performed on a Vario EL elemental analysis instrument (Elementar Co.). UV−vis absorption spectra was recorded on an UV-3600 spectrophotometer. Cyclic voltammetry was carried out on a CHI660A electrochemical work station with platinum electrodes at a scan rate of 50 mV s^{-1} against an Ag/Ag^{+} reference electrode with a nitrogen-saturated solution of 0.1 M tetrabutylammonium hexafluorophosphate (Bu_4NPF_6) in anhydrous acetonitrile. Potentials were referenced to the ferrocenium/ferrocene couple by using ferrocene as an internal standard. The deposition of a copolymer on the electrode was done by the evaporation of a dilute chlorobenzene (CF) solution.

Grazing incidence wide-angle X-ray scattering

Grazing incidence wide-angle X-ray scattering (2D-GIWAXS) experiments were carried out on a Xenocs Xeuss 2.0 system with an Excillum MetalJet-D2 X-ray source operated at 70.0 kV, 2.8570 mA, and a wavelength of 1.5405 Å. The grazing-incidence angle was set at 0.20 °C. Scattering pattern was collected with a Dectris Pilatus3R 1M area detector.

Fabrication of organic solar cell (OSC)

Solar cells were fabricated in a conventional device configuration of ITO/PEDOT:PSS/active layer/ETL/Ag. The ITO substrates were first scrubbed by detergent and then sonicated with deionized water, acetone and isopropanol subsequently, and dried overnight in an oven. The glass substrates were treated by UV-ozone for 15 min before use. The PEDOT:PSS was spin-cast onto the ITO substrates at 3200 rpm for 40 s, and then dried at 150 °C for 20 min in air. The PFBT4T-T20:NFA blends were dissolved in toluene. The blend solution was spin-cast at 2300 rpm for 40 s. Subsequently, the casted blend films with thickness of ~100 nm were annealed at 130 °C for 5 min. A thin PNDIT-F3N-Br layer was coated on the

active layer. A 100 nm Ag layer was subsequently evaporated through a shadow mask to define the active area of the devices (5.8 mm^2) and form the top anode. The PCEs were determined from *J-V* curve measurements (using a Keithley 2400 source meter) under a 1 sun, AM 1.5 G spectrum from a solar simulator (Oriel model91192; 1000 Wm^{-2}). The solar simulator illumination intensity was determined using a monocrystal silicon reference cell (Enlitech-SRC-2020) calibrated by the National Renewable Energy Laboratory (NREL). Theoretical J_{sc} values obtained by integrating the product of the EQE (QE-R3011) with the AM 1.5 G solar spectrum agreed with the measured value to within 5%.

Supplementary Figure

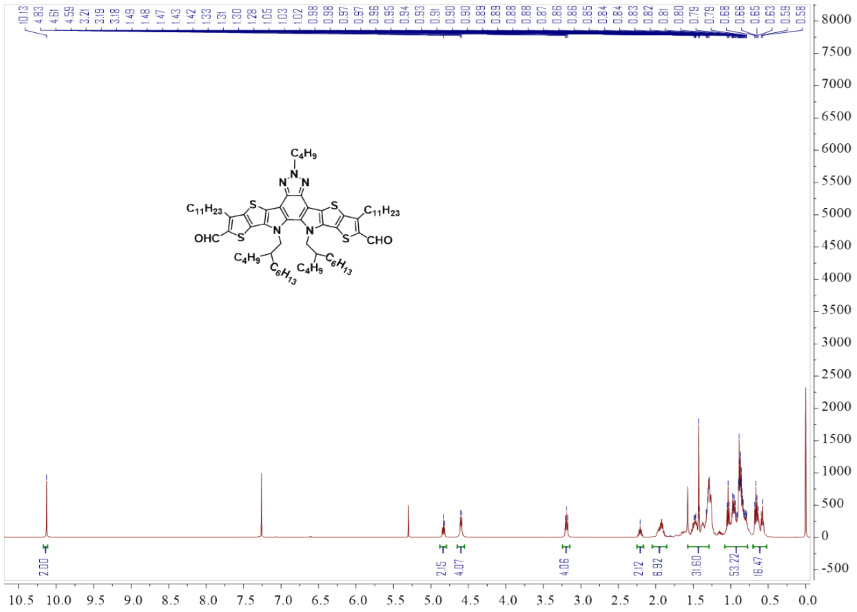

Fig. S1. ^1H NMR spectrum of **BTz-C_4C_{12}-2CHO** in $CDCl_3$.

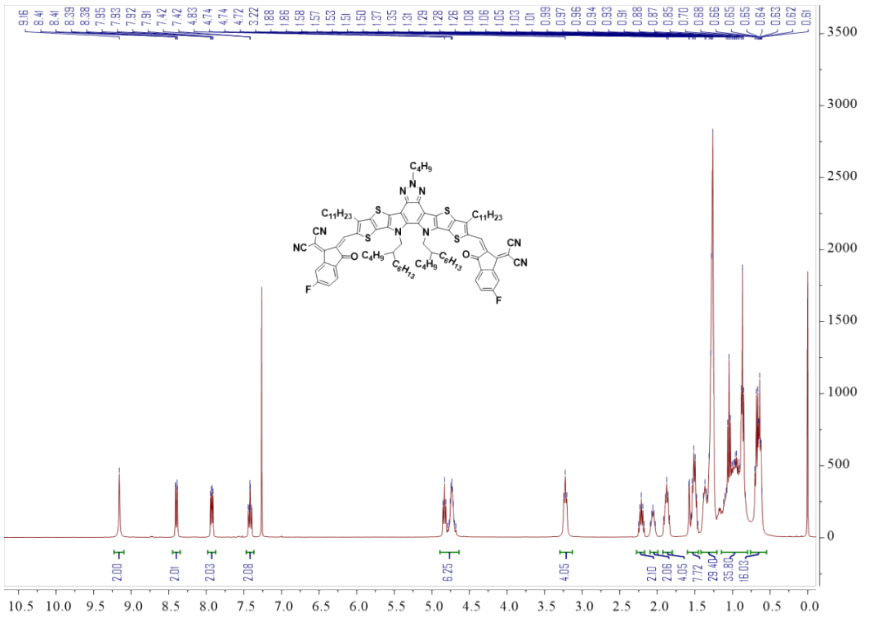

Fig. S2. ^{1}H NMR spectrum of **BTz-*δ*-C$_4$C$_{12}$** in $CDCl_3$.

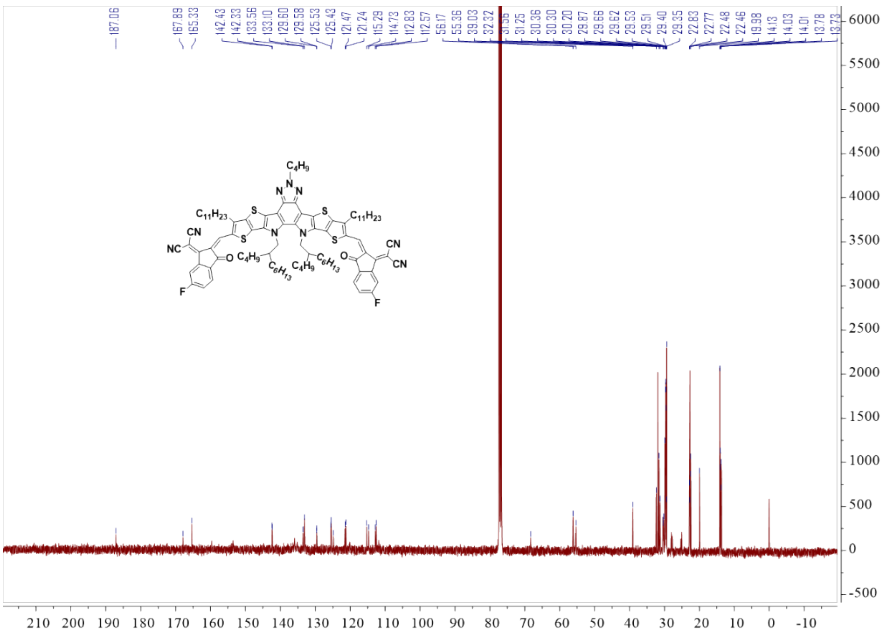

Fig. S3. ^{13}C NMR spectrum of **BTz-*δ*-C$_4$C$_{12}$** in $CDCl_3$.

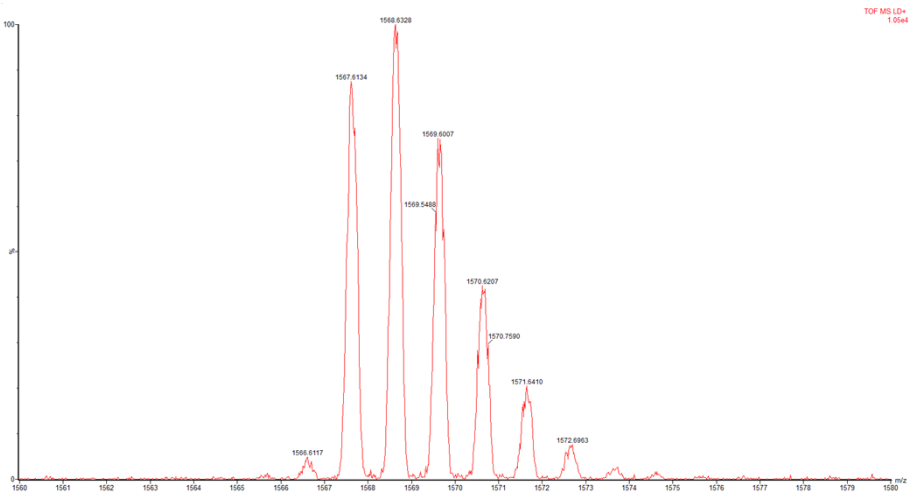

Fig. S4. The MALDI-TOF MS plot of **BTz-*δ*-C_4C_{12}** in $CDCl_3$.

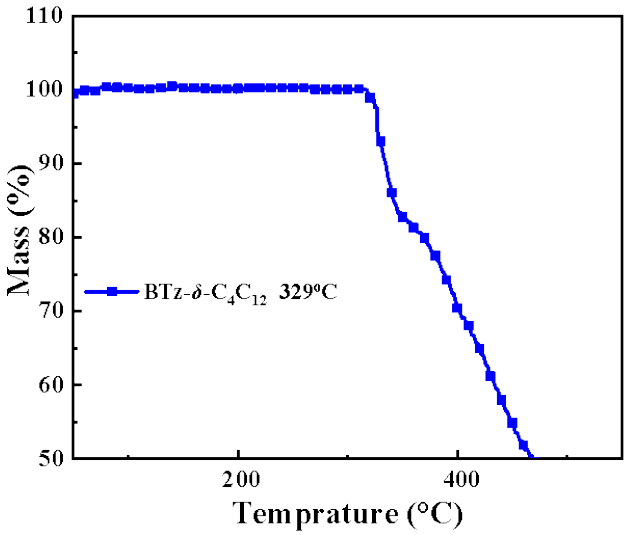

Fig. S5. TGA curves of **BTz-*δ*-C_4C_{12}**.

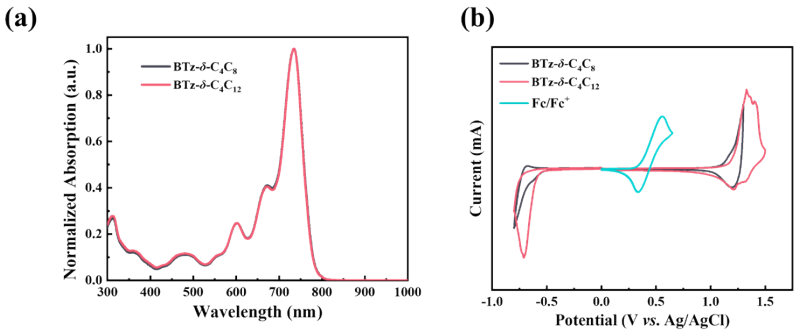

Fig. S6. (a) Normalized absorption spectra of two acceptors in dilute solution. (b) CV curves of two acceptors.

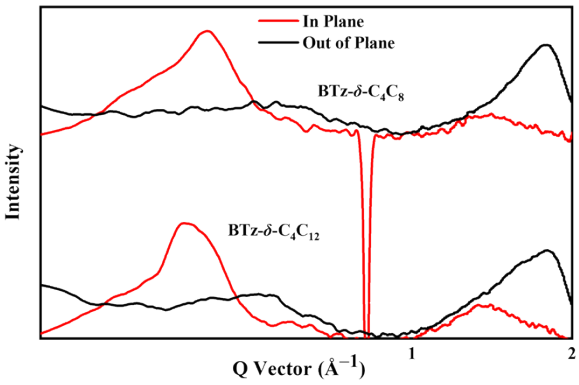

Fig. S7. The out-of-plane (black line) and in-plane (red line) line-cut profiles of the GIWAXS patterns .

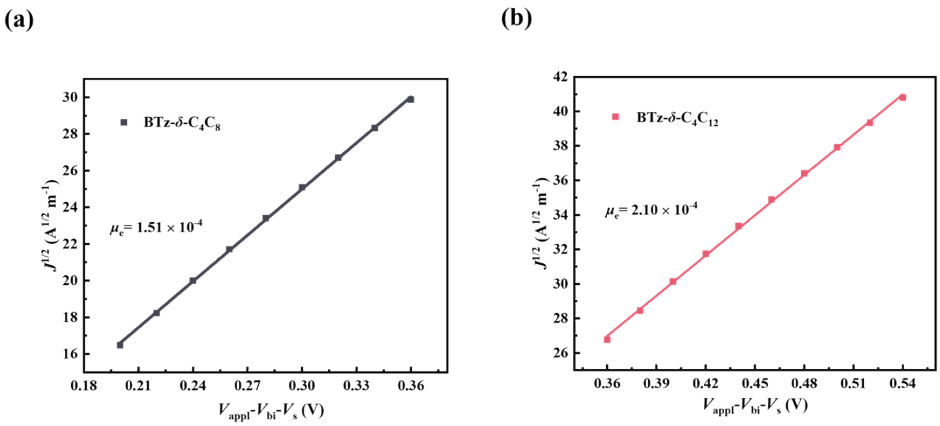

Fig. S8. (a and d)SCLC $J_{0.5}$-V characteristics of electron-only devices of NFAs pure films.

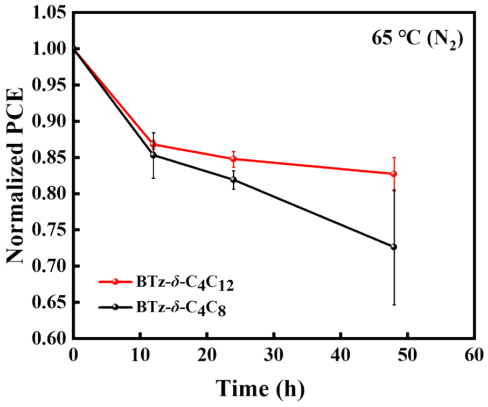

Fig. S9. The thermal stability of the PFBT4T-T20:BTz-δ-C_4C_8 and PFBT4T-T20:BTz -δ-C_4C_{12}-based devices.

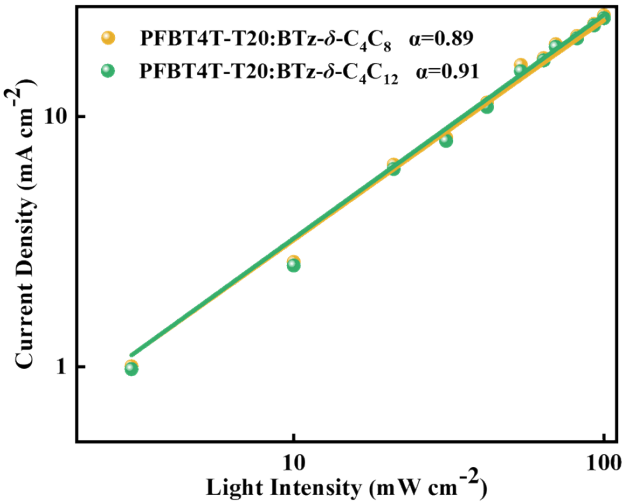

Fig. S10. Experimental J_{sc} versus light intensity of the PFBT4T-T20:BTz-δ-C_4C_8 and PFBT4T-T20:BTz-δ-C_4C_{12}-based devices.

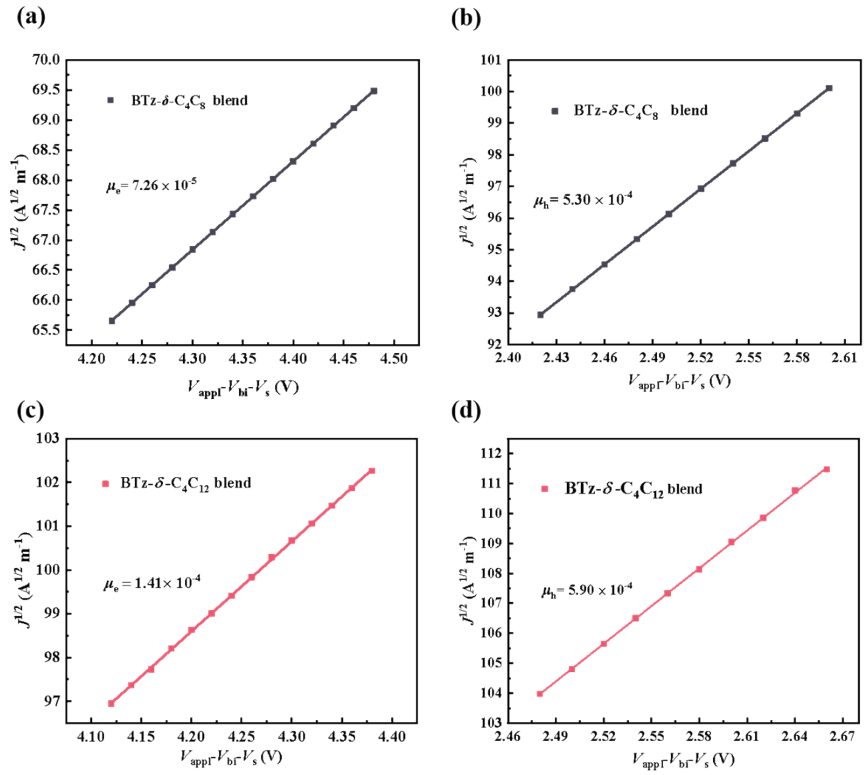

Fig. S11. (a and c) SCLC $J_{0.5}$-V characteristics of electron-only devices of blend films. (b and d) SCLC $J_{0.5}$-V characteristics of hole-only devices of blend films.

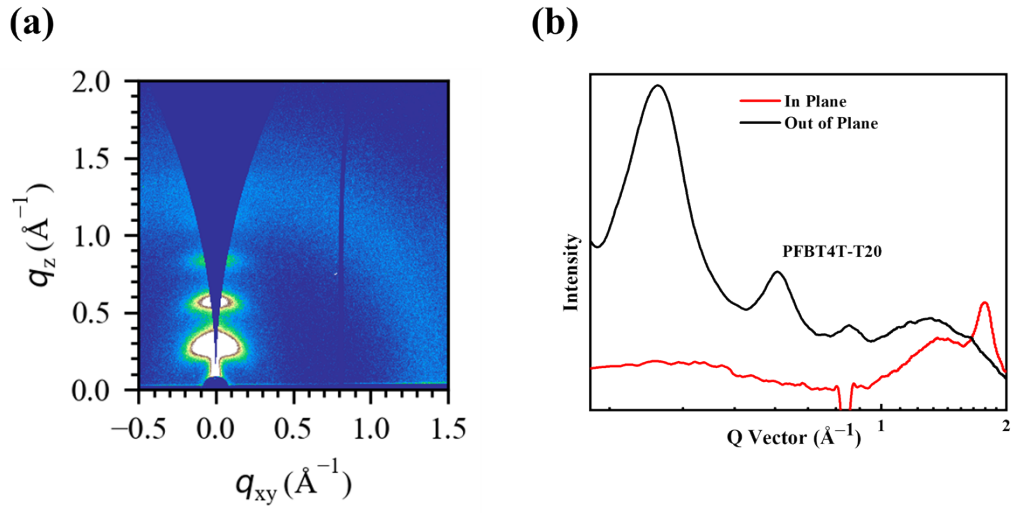

Fig. S12. (a) 2D-GIWAXS pattern images of PFBT4T-T20 pure film. (b) The out-of-plane (black line) and in-plane (red line) line-cut profiles of the GIWAXS patterns.

Supplementary Table

Table S1. Electrochemical properties, optical absorption in solution and in solid film, of the three acceptors.

Film	λ_{max}		λ_{onset}	E_g^{opt}	HOMO	LUMO
	Solution [nm]	Film [nm]	[nm][a)]	[eV][b)]	[eV]	[eV]
BT-δ-C_4C_8	734	853	956	1.30	–5.53	–3.84
BT-δ-C_4C_{12}	734	861	969	1.28	–5.55	–3.80

a) Obtained with the film. [b)] Optical bandgap calculated from 1240/λonset (eV).

Table S2.GIWAXS characteristics of three acceptors films for *q* vector, *d*-spacing, crystal coherence lengths and number of stacked layers (*n*).

Materials	OOP(010)				IP(100)			
	q(Å^{-1})	π–π spacing(Å)	L_c(Å)	*n*	q(Å^{-1})	d-spacing(Å)	L_c(Å)	*n*
BT-δ-C_4C_8	1.78	3.53	22.0	6.2	0.41	15.32	84.6	5.3
BT-δ-C_4C_{12}	1.79	3.51	18.3	5.2	0.37	16.97	112.3	6.6

Table S3. Surface energy (γ_s) and Flory-Huggins interaction parameter(χ) of all films.

Film	Contact angle (°)		γ^d	γ^p	γ_s	χ_{D-A}
	θ_{water}	θ_{oil}	[mN/m]	[mN/m]	[mN/m]	[k]
PFBT4T-T20	101.3	53.6	31.91	1.74	33.65	–
BT-δ-C_4C_8	97.5	38.8	38.76	1.94	40.70	0.34k
BT-δ-C_4C_{12}	94.1	41.8	36.36	3.49	39.85	0.26k

Table S4. Photovoltaic parameters of the donor:BTz-*δ*-based on devices.

donor	V_{oc} (V)	J_{sc} (mA cm^{-2})	FF (%)	PCE (%)
D18	/	/	/	/
PM6:BTz-δ-C_4C_8	0.853	18.17	61.99	9.60
PM6:BTz-δ-C_4C_{12}	0.858	19.40	65.22	10.85

Table S5. Photovoltaic parameters of the ten optimized PFBT4T-T20:BTz-δ-C_4C_8 based on devices.

Number	V_{oc} (V)	J_{sc} (mA cm^{-2})	FF (%)	PCE (%)
1	0.782	24.3	72.8	13.8
2	0.772	25.8	72.3	14.4
3	0.782	24.7	74.2	14.3
4	0.782	25.6	71.2	14.3
5	0.782	24.8	69.5	13.4
6	0.792	25.2	72.9	14.5
7	0.782	25.5	73.8	14.7
8	0.782	25.0	74.0	14.4
9	0.782	25.5	71.5	14.3
10	0.792	25.4	72.0	14.5

Table S6. Photovoltaic parameters of the ten optimized PFBT4T-T20:BTz-δ-C_4C_{12} based on devices.

Number	V_{oc} (V)	J_{sc} (mA cm^{-2})	FF (%)	PCE (%)
1	0.784	27.5	76.7	16.6
2	0.782	27.3	76.7	16.4
3	0.784	27.34	75.5	16.3
4	0.781	26.8	76.1	16.1

5	0.784	27.6	74.8	16.2
6	0.784	27.5	74	16
7	0.783	27.4	76.1	16.4
8	0.784	27.5	75.5	16.3
9	0.784	27.6	76.7	16.5
10	0.784	26.3	75.7	15.6

Reference

1 M. Luo, L. Kong, J. Liang, Z. Zhang, S. Deng, L. Zhang, X. Qiao, D. Ma, J. Chen, *Chem. Eng. J.* 2023, **457**, 141281.